Low Power and High Gain Double-Balanced Mixer dedicated to 77 GHz Automotive Radar Applications

A. Mariano, T. Taris, B. Leite, C. Majek, Y. Deval,
E. Kerhervé, J-B. Bégueret
IMS Laboratory – University of Bordeaux
Bordeaux – France
andre.mariano@ims-bordeaux.fr

D. Belot
Innovation & Collaborative Research
STMicroelectronics
Crolles, France

***Abstract*—In this paper, we present a mixer implemented in a 130 nm BiCMOS technology dedicated to 77 GHz automotive radar applications. The architecture is based on a double-balanced Gilbert cell with integrated transformer-based Baluns. Interconnections between devices, capacitor accesses and Tee-junctions are modeled using EM software in order to improve the simulation accuracy. The measurement results of the circuit exhibit a conversion gain and a SSB noise figure of 18.5 dB and 13.8 dB respectively over a 74 to 81 GHz band. Supplied under 2.5 V the power consumption is 80 mW and the ICP1 is -13 dBm. The transformer-based Balun allows a good input matching at the RF input port over a 16 GHz range from 72 to 88 GHz.**

I. INTRODUCTION

Recent improvements in SiGe BiCMOS technologies result in high speed transistors, achieving transition frequency beyond 200 GHz. Hence III-V devices are nowadays challenged by silicon-based technologies, allowing low-cost implementation of millimeter-waves (mmW) systems as radar sensors for the automotive industry [1-2].

Next car generations are expected to be more safety. To do so a combination of short and long range RADAR modules will surround the automobile. To address these two applications a frequency band of 76 to 81 GHz must be covered. Focusing on the receiver part of RADAR modules this work proposes the design and implementation of a mm-Waves mixer suitable for the two scenarios.

The most popular mixer topology is the fully balanced Gilbert cell [3]. It provides a large conversion gain, a high linearity and a good reverse isolation, which are characteristics really mandated in RADAR applications. The design flow of such building block is well defined in RF domain but its implementation in a silicon technology for mm-Waves applications is challenging. A second point of interest is the 6 GHz bandwidth to be covered which requires a specific design approach. These two points are particularly addressed in this work. The design flow of the mixer core and the single-ended to differential converter are first reviewed. The third section proposes a systematic modeling of device interconnects and accesses allowing a better anticipation of the overall circuit behavior. The experimental results are then discussed and compared to the state of art in the last part.

II. CIRCUIT DESIGN

The block diagram of the proposed mixer is depicted in Figure 1. The core is based on a double-balanced active topology (Gilbert cell) [3]. Two integrated Baluns are implemented to convert the single-ended to differential signal at the RF and LO ports. The output differential signal, IF port, is recombined into a single-ended termination for measurement purpose by an off-chip Balun.

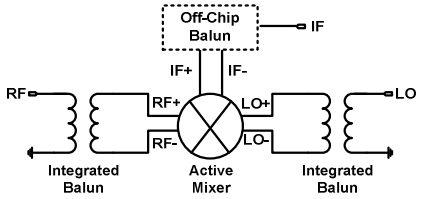

Figure 1. Block diagram of the proposed double-balanced active mixer

A. Balun Design

A basic inductive degeneration is usually implemented to perform input matching in the transconductance stage. But this narrow band approach is not suited here to cover the 6 GHz targeted bandwidth. One solution is to associate the inductive degeneration with a transformer-based converter which presents intrinsic wideband impedance. According the Figure 2 the Baluns are routed with the two top thick metal layers. A stacked topology with octagonal shape turn was selected since it is less lossy than interleaved and square transformers [4]. The primary and secondary access lines are located on opposite sides of the transformer (flipped topology) and the primary is center-tapped to match the mixer layout. Each winding exhibits a single octagonal turn with an average diameter of 70 µm and a trace width of 4.4 µm. Figure 3 shows the close agreement between EM simulated and measured phases for both differential ports of the Balun. The

phase difference between these ports shows little deviation from the desired 180 degrees over the considered frequency band.

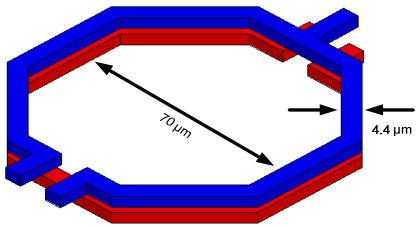

Figure 2. HFSS layout of the transformer-based Balun

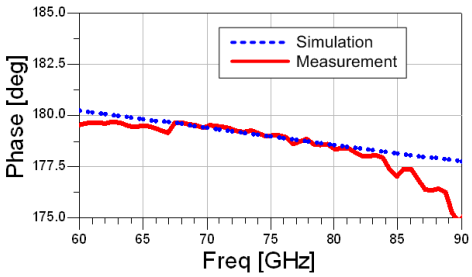

Figure 3. Comparison between the simulated and measured phases for the differential ports of the Balun

B. Gilbert cell design

The Figure 4 depicts a simplified schematic of the mixer core which consists in a transconductance stage (T_1,T_2) which converts the input RF voltage into current and a switching stage (T_3 – T_6), that commutates the RF current between the two output IF nodes. The matching between the input stages and the Baluns are performed by the AC coupling capacitors, C_1 and C_2, combined with the T-Lines TL_1 and TL_2, respectively. The biasing voltages Vb_{LO} and Vb_{RF} are provided by two current mirrors. The TL_3 lines degenerating the emitter of (T_1,T_2) linearize the RF input stage. A trouble node in a fully balanced topology is the connecting point between the transconductor and switching stages. Indeed the parasitic capacitors contribute to lower both the isolation between LO and RF ports and the conversion gain (CG). This phenomenon increasing with the operating frequency is compensated here by an inter-stage matching TL_4 which resonates with the local parasitics at the RF frequency.

The sizing of T_1 and T_2 is led by the optimal current density for a large gain. The CG of a Gilbert cell can be expressed as reported in equation 1. It increases with the improvement of I_{mixer} current and R_c. They are fixed to 12 mA and 115 Ω.

$$CG = \frac{2}{\pi} . g_{m_{1/2}} . R_c \qquad (1)$$

Considering that the switching is almost perfect which means (T3 – T6) are as small as possible, the NF is mainly supported by the transconductor stage. To reduce the NF, the base-emitter area as well as the number of fingers are set large.

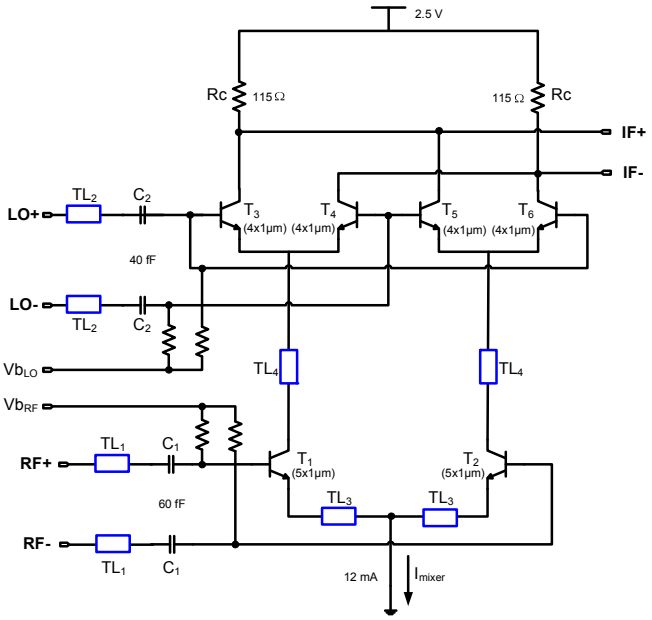

Figure 4. Double-balanced mixer topology

III. CONSIDERATIONS FOR DESIGN IMPLEMENTATION

Operating at 80 GHz, the wavelength of the signal, roughly 1 mm, is in the range of the circuit (0.57 mm^2). As a matter of consequence, interconnections and metal path rather behave like distributed devices than mere RC type elements. To address this point, customized models were developed, using T-Lines available in the Design Kit.

1) Layout interconnections can be modeled as T-Lines of corresponding metal levels and geometries. An example, concerning the connection between two lumped resistors, is reported in Figure 5.

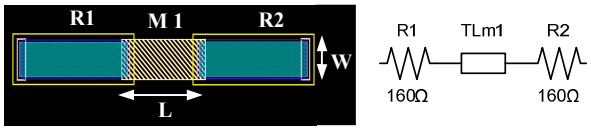

Figure 5. Interconnection between two resistors (a) modeled as a T-line (b). All interconnections must be modeled and included in simulations.

2) MIM capacitors terminations must be considered as Aluminum (AP)/Metal6 (M6) T-Lines and modeled consequently. An example, relative to a 3pF capacitor, is depicted in Figure 6.

3) RF pads are divided into two parts following an ideal line across the center wherein the test probe is located as shown in Figure 7. Likewise MIM capacitors, a T-line models the connection between the probe and the circuit, whereas an open T-line represents the outer side of the Pad. Concerning the DC pad contribution, it can be neglected if enough DC decoupling is provided.

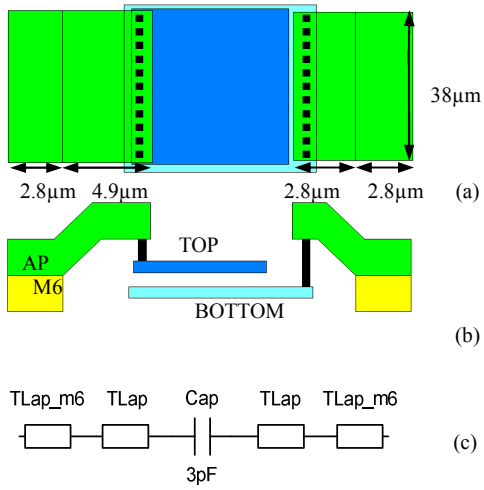

Figure 6. 3pF MIM capacitor area (a), section (b), and its equivalent model (c). Capacitor terminals are represented as T-Lines.

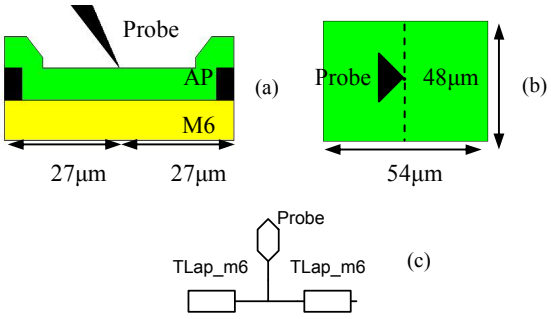

Figure 7. RF Pad section (a), area (b), and its equivalent model (c). Pads are modeled as two T-Lines, one on each side of the test probe.

IV. Experimental Results

The chip microphotograph is shown in Figure 8. It takes place within a 0.57 mm^2 including pads and Baluns. The circuit was manufactured in a 130nm SiGe:C BiCMOS technology. All measurements were done on wafer at 20°C with 110 GHz ground-signal-ground (GSG) probes. The mixer core supplied by a 2.5 V consumes 32 mA.

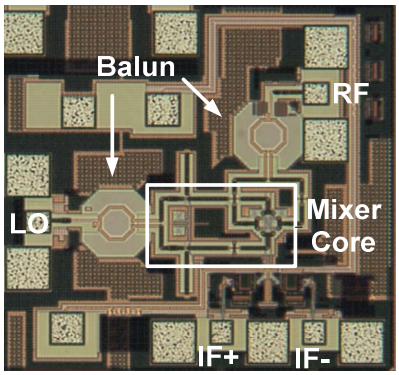

Figure 8. Microphotograph of the double balanced mixer

The RF (75 – 80 GHz) and LO (80 GHz) signals are provided by an Agilent PNA network analyzer E8361A and an Agilent PSG signal generator E8257D, respectively. The IF output is collected using an Agilent PSA spectrum analyzer E4440A via an external differential to single-ended Balun. The measured conversion gain as a function of the RF frequency is presented in Figure 9. For this measurement, the LO frequency and power are set to 80 GHz and +1 dBm. The CG varies from 17.2 – 18.5 dB with a maximum at 77 GHz. Most of the 1.3 dB ripple is introduced by the variable attenuator inserted between the LO port and the PSG generator.

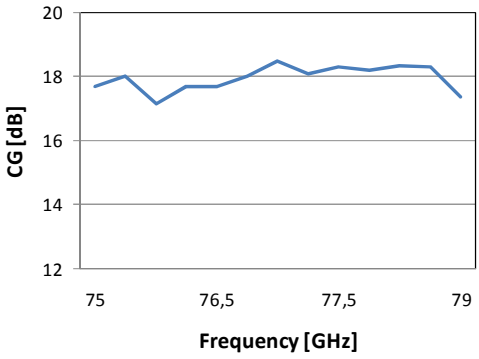

Figure 9. Measured CG as a function of RF frequency (plo = +1 dBm)

The noise figure was characterized using a noise source NoiseCom NC5110 and a HP8970B noise figure. The measured conversion gain and single side band noise figure (NF_{SSB}) as a function of LO power are reported in Figure 10. We observe that both characteristics improve with the LO power and saturate for LO value exceeding +1 dBm. Under such conditions, the lower value of NF, 13.8 dB, is obtained. According to section II, the NF of the mixer core can be improved by changing the current density in the transconductance stage thus scarifying CG for NF. The losses in the input Balun which are estimated to 5.5 dB contribute to worsen the overall NF. Deembedding its participation by Friis formula, the noise figure of the mixer core is assessed at 8.3dB.

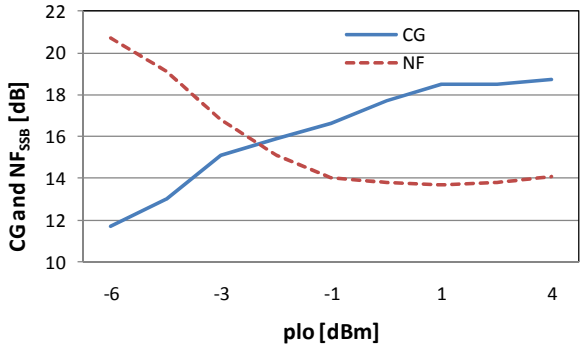

Figure 10. Measured CG and NF_{SSB} as a function of LO power (f_{RF} = 77 GHz and f_{LO} = 80 GHz)

The linearity has been evaluated by measuring the input-referred compression point (ICP1). The IIP3 was not tested since no equipment could provide the adequate two tones test. Figure 11 shows the plot of the IF output power as a function

of the RF input power. In this measurement, the RF and LO frequency are 77 GHz and 80 GHz, respectively. The LO power was set to +1 dBm. The circuit achieves an ICP1 of -13 dBm thanks to the TL_3 degeneration. Almost the same values are obtained varying the LO frequency from 78 to 82 GHz which corresponds to an IF frequency sweeping from 1 to 5 GHz. The upper limit of the IF band is limited by the output matching bandwidth of the buffer.

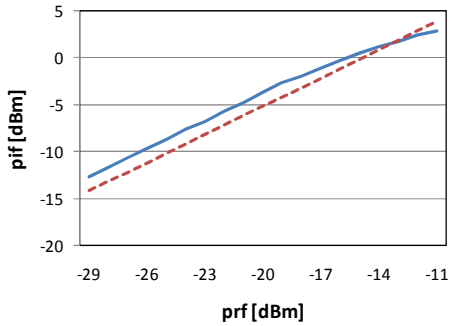

Figure 11. Measured ICP1 (f_{RF} = 77 GHz, f_{LO} = 80 GHz and plo = +1 dBm)

The RF and LO input matching was measured employing an Agilent PNA network analyzer E8361A. They are reported in the Figure 12. They present a return loss lower than -10 dB from 72 to 88 GHz for RF port and from 77 to 86GHz for LO port. These wideband performances are mainly supported by the integrated transformer-based Baluns.

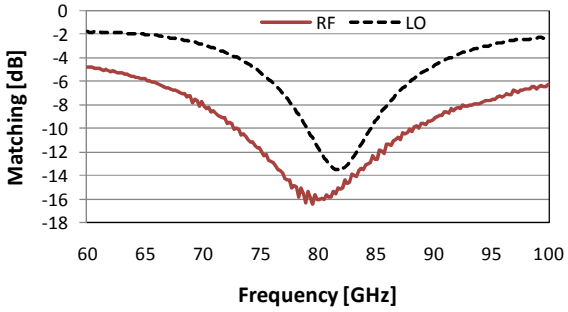

Figure 12. Measured RF and LO input matching

Table I summarizes the measurement results of the reported circuit and others realizations within the 77 to 80 GHz range. The proposed mixer exhibits the second higher conversion gain and the lowest power consumption. The overall characteristics can be compared through the Figure Of Merit (FOM) defined in equation 2.

$$FOM = 10\log\left(\frac{10^{G/20}.10^{ICP1/20}}{10^{NF/10}.P_{DC}.V_{cc}}\right) \quad (2)$$

Note that the best FOM is the one closest to 0 dB, ref. [5] in this case. The proposed mixer performs a good trade-off between the considered characteristics, presenting the second best reported FOM. To the knowledge of the authors the power consumption of the circuit is the lowest reported in the literature.

TABLE I. SUMMARY OF 77GHZ MIXER PERFORMANCES

Ref.	NF_{SSB} [dB]	CG [dB]	ICP [dBm]	Vcc [V]	P_{DC} [mW]	FoM dB[$V^{-2}.A^{-1}$]
[5]	11.2	15	2.5	5.5	335	-33.85
[6]	14	24	-30	-5	300	-63.76
[7]	16.5	11	0	5.5	413	-44.56
[8]	18.4	13.4	-12	4.5	176	-52.69
[9]	16	15.5	-3	5.5	187	-41.37
This work	13.8	18.5	-13	2.5	80	-40.56

V. CONCLUSION

A low power and high conversion gain double-balanced mixer dedicated to 77 GHz automotive RADAR applications is presented. Transformer-based Baluns have been implemented on-chip in order to improve the input matching bandwidth and convert the single-ended inputs to differential. The proposed mixer presents a good trade-off between gain, noise figure and power consumption. It reaches a measured conversion gain and a SSB noise figure of 18.5 dB and 13.8 dB respectively over a 74 to 81 GHz range. The power consumption is only 80 mW under 2.5V and the ICP1 is -13 dBm for a RF frequency of 77 GHz.

REFERENCES

[1] S. Voinigescu *et al.*, "Comparison of Silicon and III-V Technology Performance and Building Block Implementations for 10 and 40 Gb/s Optical Networking ICs", in JHSES, vol. 13, pp. 27-57, Mar. 2003.

[2] P. Chevalier, et al, "High-Speed SiGe BiCMOS Technologies:120-nm Status and End-of-Roadmap Challenges," IEEE SiRF, pp.18-23, Jan07.

[3] B. Gilbert, "A Precise Four-Quadrant Multiplier with Subnanosecond Response," IEEE Journal of Solid State Circuits, vol. SC-3, N4, pp. 365-373, December 1968.

[4] B. Leite, E. Kerherve, J. B. Begueret, and D. Belot, "Transformer topologies for mmW integrated circuits," in IEEE Proc. 39th European Microwave Conference, Rome, Italy, 2009, pp. 181 – 184.

[5] Trotta, S., Dehlink, B., Knapp, H., Aufinger, K., Meister, T.F., Bock, J., Simburger, W., Scholtz, A.L., "Design considerations for low-noise, highly-linear millimeter-wave mixers in SiGe bipolar technology", ESSCIRC 07, pp. 356 – 359, Sept. 2007.

[6] W. Perndl, H. Knapp, M. Wurzer, K. Aufinger, T. Meister, J. Böck, W. Simbürger, and A. L. Scholtz, "A low-noise and high-gain doublebalanced mixer for 77 GHz automotive radar front-ends in SiGe bipolar technology," IEEE RFIC Digest, pp. 47–50, June 2004.

[7] B. Dehlink, H.-D. Wohlmuth, H. Forstner, H. Knapp, S. Trotta,K. Aufinger, T. Meister, J. Böck, and A. L. Scholtz, "A highly-linear SiGe double-balanced mixer for 77 GHz automotive radar applications," IEEE RFIC Digest, pp. 235–238, June 2006.

[8] L. Wang, R. Kraemer, and J. Borngraeber, "An improved highly-linear low-power down-conversion micromixer for 77 GHz automotive radar in SiGe technology," IEEE MTT–s Digest, pp. 1834–1837, June 2006.

[9] T. O. Dickson, M. A. LaCroix, S. Boret, D. Gloria, R. Beerkens, and S. P.Voinigescu.,"30-100-GHz inductors and transformers for millimeter-wave (Bi)CMOS integrated circuits," IEEE Transactions on Microwave Theory and Techniques, vol. 53, no. 1, pp. 123–133, Jan. 2005.